Proceedings of IMECE2002
ASME International Mechanical Engineering Congress & Exposition
November 17–22, 2002, New Orleans, Louisiana

IMECE2002-39587

NUMERICAL AND EXPERIMENTAL STUDY OF IMPELLER DIFFUSER INTERACTION

Tarek Mekhail (Ph.D)
Du Zhaohui (Professor)
Willem Jansen (Guest Professor)
Chen Hanping (Professor)
Shanghai Jiao Tong University,China

ABSTRACT

The unsteadiness of the flow at the leading edge of a vaned diffuser represents a source of low efficiency and instability in a centrifugal turbomachine. Furthermore, the internal flow of the impeller can be affected by asymmetric downstream conditions, which results in extra flow unsteadiness and instabilities. Numerical and experimental data are obtained. The simulation of impeller diffuser interaction is performed using CFX-Tascflow. A frozen rotor simulation is used for the steady calculation and a rotor-stator simulation is used for the unsteady calculation using the steady results as an initial guess. The unsteady simulation is done not only for one impeller and diffuser blades, but also for the whole impeller and diffuser blades using Unix workstation. For the experimental work, a transparent fan is design and tested at The Turbomachinery Laboratory of SJTU. The test rig consists of a centrifugal, shrouded impeller, diffuser and volute casing all made of plexiglass. A particle image velocimeter (PIV) is used to measure the 2-D instantaneous velocity in the interaction region between impeller, vaned. A series of performance measurements were carried out at different speeds. The first trial of measuring the instantaneous flow field in a part of the impeller and vaned diffuser together at different relative locations between them is presented in this work at different flow rates. Obtaining detailed measurements in the interaction region between the impeller and diffuser can help in understanding the complex flow phenomena and improving centrifugal fan and compressor performance. Finally, the comparison between the unsteady measurements and unsteady calculations showed that the Rotor/Stator Model can predict the basic characteristics of unsteady flow in centrifugal fan but still need improvement to satisfy the true transient simulation for unsteady impeller diffuser interaction

INTRODUCTION

The improvement of machine performances can only be achieved if there is a progress in the comprehension of the nature of the complex flow that develops at the gap between rotor and stator. During the design of a turbomachine, the flow is considered steady and uniform at the entry of each element. For a centrifugal fan with a vaned diffuser, satisfying this assumption requires a large interface between the rotor and the stator so that the mixing process of the flow leaving the impeller can take place. Otherwise, the unsteady flow that enters the diffuser represents a source of low efficiency. Furthermore, the internal flow of the impeller can be affected by asymmetric downstream conditions, which results in extra flow unsteadiness and instabilities. A number of authors have treated the problem of the interaction of the impeller and its surroundings. Inoue and Cumpsty [1], Sideris [2] and Arndt [3,4] have been concerned with the action of the diffuser. A large number of the experimental investigations that revealed the presence of jet-wake structure at the discharge of centrifugal rotors was done by Eckardt [5, 6], and more recently Rohne [7] and Ubaldi [8]. However, Krain [9] found a velocity profile that differed widely from the jet-wake type flow. Paone at al. [10], at VKI have used (PIDV) to measure the flow field inside the vaneless diffuser of a centrifugal pump made of plexiglass with a shrouded impeller. They compared the (PIDV) measurements and the corresponding (LDV) and found that they are different in the wake. They believed that the information available from (PIDV) could largely contribute to a better understanding of the flow in centrifugal machines. Humphreys and Bartram [11] from NASA Langley Research Center described the different constituent components of PIV system and different challenges affecting each component of the system. e.g., flow seeder, laser

optics system image shifter and camera system. Methods used to overcome these obstacles were described and several examples of the use of PIV are given to illustrate some of the choices and solutions available to the system designer. Warnet [12] Made a successful PIV measurements in the vaneless space (between impeller blades and diffuser blades) of high-speed centrifugal impeller. Instantaneous flow measurements were also obtained during compressor surge. Among those papers presented above, and many others, no one has measured the unsteady flow field in the interaction region between impeller and diffuser and compared it to the calculated. Therefore, the present work introduces the instantaneous flow field in the interaction region for both impeller and diffuser together at different relative locations between them using PIV and compared them to the calculated one using CFX-Tascflow. The detailed of measurements and the test rig can be found in Mekhail et.,al.[13,14]

NUMERICAL TECHNIQUE

A high quality mesh is produced using a single block H-grid through the main blade and the passage using CFX-Turbogrid software. This type of grid for this problem gives better minimum skew angle, which should not be less than 20 degree, and better maximum aspect ratio, which should not be more than 100. The blades are defined by blocking off grid elements. The entire grid size for one blade is:

For the impeller

Entire grid: 42*32*23=30912 (streamwise, circumferential, spanwise)

Blade block off 24*8*23=4416

For the vaned diffuser

Entire grid: 46*27*23=28566 (streamwise, circumferential, spanwise)

Blade block off 22*5*23=2530

Figure 1 shows the grid of the impeller, vaned diffuser and the sliding plane. The total number of grid nodes is around 750,000 nodes for the whole impeller and diffuser blades.

TRANSIENT ROTOR/STATOR AND FROZEN- ROTOR SIMULATION

The frozen rotor simulation is used to get the steady state solution for different components of the machine i.e., the type of the interface condition is steady state and fixed relative position across the interface. There are several differences between the Frozen Rotor and transient rotor/stator parameters:

1. **Timestep:** The timestep for the Frozen Rotor simulation is large relative to the transient simulation. In the Frozen Rotor simulation a steady state answer is desired, thus a large timestep is chosen. In the transient simulation a timestep small enough to resolve the transient effects of interest must be used (often a small fraction of omega).
2. **Iteration:** For a transient simulation, it is generally recommended that iteration within each timestep be performed. In the case of transient rotor/stator it is critical that (some) iteration be performed each timestep, since the domain geometry is changing with each timestep.
3. **Output:** For the transient simulation, data must be saved to a disk each timestep, so that the transient result can be postprocessed.

A transient rotor/stator simulation can be used any time it is important to account for transient interaction effects at a sliding (frame change) interface. By the nature of this kind of interface, these simulations are always transient, never achieving a steady state condition. The components on each side of a transient sliding interface are always in relative motion with respect to each other. Pitch change is automatically dealt with at a transient sliding interface in the same manner as at Frozen Rotor interfaces: the profiles in the pitch-wise direction are stretched or compressed to the extent that there is pitch change across the interface. All flows (mass, momentum, energy etc.) are scaled accordingly, based on the pitch change. As with the Frozen Rotor condition, the computational accuracy degrades rapidly with increasing pitch change. It is recommended that sufficient blade components be analyzed on each side of the transient sliding interface to minimize pitch change.

BOUNDARY CONDITIONS AND SOLUTION PROCEDURES

The velocity is specified over the entire inlet face. The outlet flow condition is set as the outlet measured static pressure applied as an average value over the outlet area of the diffuser. The diffuser is stationary and the impeller is rotating with a rotational speed of 1000 rev/min. Additionally, in the K-ε turbulence model in Tascflow requires an inlet value for the turbulence intensity (Tu) and the eddy length (L). Most of the computations for the present work were run in fully turbulent mode with Tu=5 percent and L=0.005 and the Reynolds number is 4.5E4. The frozen rotor simulation is obtained first using a larger time step (Δt=E-3 sec). The transient simulation is done using smaller time step (Δt=1.5E-4) with using the frozen rotor simulation as an initial guess. The number of iteration per time step is 15. The simulation is obtained for one impeller and diffuser blade then, the grids are appended to get the whole impeller and diffuser blades and passages. The calculation results discussed here were run on UNIX workstation with 512 Mbytes of memory, which can be extended to a virtual memory of 1Gbyte. Typical CPU times were around 16 hours for 200 iterations for frozen rotor simulation and 3 days for 60 iterations for transient simulation necessary for a run to converge down to maximum residuals of less than E-05.

RESULTS AND DISCUSSION

1. Frozen Rotor Simulation

The predicted impeller flow exhibits, by the exit from the blade, the development of the jet-wake structure. Figure 2 shows a relief plot of the steady state-predicted meridional flow velocity normalized by impeller tip speed (C_{mer}/U_2) at the exit

plan of the impeller at medium flow rate. C_{mer} calculated from the equation:

$$C_{mer} = \sqrt{U_{mer}^2 + V_{mer}^2 + W_{mer}^2}$$

The figure shows that a clear jet (of high meridional flow velocity) at the pressure side and a wake (of lower velocity) near hub suction side. Also, the disturbed flow near the suction side shows that there is another low velocity region, near the shroud side but not very close to the suction side.

Figure 3-a and b shows the symmetric flow streamlines and velocity vectors in meridional symmetric plane (at mid pitch between the pressure side and the suction side) for impeller and vaned diffuser. As the rotational speed is small, the figure shows that no separation occurs in the impeller at the meridional symmetric plane. The absolute meridional velocity vector near the impeller shroud is higher than that near the hub. For the diffuser, the figure shows a detached flow closes to the hub at nearly 40 percent of the diffuser. The hub detachment seems to arise from a disturbance generated at the moving impeller hub/stationary diffuser wall interface. The question is why the flow separates at the hub and not separates at the shroud?. The answer is simply comes from Newton's third law "Action and reaction are equal and opposite". The action is the inflow to the impeller and the reaction is the separating flow at the hub of the diffuser and it occurs very far from the impeller inlet because of the centrifugal force and momentum of the fluid, i.e., the flow is trying to go to the opposite direction of the impeller inlet at the diffuser hub. The hub separation is also seen numerically (Kirtley and beach [15]) and experimentally (Hathaway[16]) for NASA Lewis Low Speed Centrifugal Compressor. The reattachment near the hub might be happened after the diffuser.

2. Transient Rotor/Stator Simulation

Unsteady phenomena generated by stator/rotor interactions are classically divided into potential effects that propagate upstream and downstream, and wake effects that are convected downstream. The potential unsteady effects -observed in the stator- are caused by the motion of the non-uniform pressure field that is steady in the rotor frame. This unsteady pressure observed in the stator is like the unsteady variation recorded by a pressure probe moving uniformly across a non-uniform, steady, pressure field generated by an isolated airfoil. Similarly, the potential effects observed in the rotor are due to the non-uniform pressure field that is steady in the stator frame. Unsteady effects generated by wake/blade interactions are due to the slicing in pieces of the wakes that are created by viscosity, issued from the impeller blades, by the downstream blade.

A huge amount of data has been obtained during a cycle of the transient simulation process. One cycle is divided into 20 timestep each timestep is 10 iterations and a converged solution has been obtained after 3 cycles (where the initial guess for the transient simulation is taken as the converged solution of the frozen rotor simulation). Due to large amount of data, all of the impeller positions could not be presented here; only one position is selected and presented for each case.

Figure 4-a,b and c shows, the evolution of the instantaneous pressure field at design flow rate near the hub, at midspan and near the shroud. The potential effect, when the impeller trailing edge passes in front of the diffuser vane leading edge, is clearly visible. Pressure perturbations due to the vortex shedding behind the impeller blades can be observed also. In the simulation a constant ambient pressure was imposed at the outlet of the diffuser (from measurement). Therefore, the outlet pressure is steady and variations are seen far from the outlet. In a small band around the vaneless gap part of the fan, complex pressure structures can be observed. These pressure structures are well correlated with the unsteady part of the relative velocity norm at the exit of the impeller. Outside this band, the pressure field is smoother and it can be observed that the pressure unsteadiness in the impeller is well synchronized. These global pressure variations are due to potential effects. It can also be noted that in the diffuser the pressure is changing with time only in the semi-vaneless space. Inside the diffuser, the pressure field is almost steady. Also, it is noted that the pressure near the shroud of the diffuser is smaller because the through flow velocity near the shroud is higher. Examining these figures again, it is noted that:

- Although the grid system is the same for every diffuser passage and the number of impeller blades is equal to the number of the diffuser blades, the pressure contours are not the same for every diffuser passage.
- This difference is due to the unsteady interaction between impeller blades and diffuser blades.
- The difference between the pressure contours is small because the rotational speed is very small and flow condition is at medium flow rate near the best efficiency point.
- The calculation is done at 60 percent of the design mass flow rate. Figure 5 shows the pressure contours at 60 percent of the design mass flow rate at midspan at two positions. As shown from the figure, the difference of pressure contours is clear and a strongly unsteady flow is found at the vaneless space.

Since the computations are performed in a rotating frame in the impeller and in a fixed frame in the diffuser, it is natural to present the velocity field for both frames. Figures 6-a,b and c shows the evolution of the instantaneous relative velocity vectors in the impeller and the absolute one in the diffuser at design flow rate near the hub at midspan and near the shroud. The evolution of the absolute velocity norm is viewed in a fixed frame. Conversely, the evolution of the relative velocity is viewed by an observed attached to the impeller. These animations give a good overview of the stator-rotor interaction mechanisms. Examining these figures, it is found that:

- Near the hub, the flow velocity is high along the impeller blade at the suction side (up to about 80% of the blade length) and it is becomes slower in the last 20% percent due to wake formation at the exit suction side and due to the blade bent at the exit. Then the flow enters the vaneless space with highly unsteady velocity and the velocity becomes very small when it reaches the diffuser blade and a large separated flow occurs in the diffuser.
- At midspan, when examining carefully behind the trailing edge of the impeller blade, a small vortex shedding can be observed and a low velocity region moves with the blade trailing edge in the vaneless space in the same direction of the diffuser blades. Also, a low velocity region is observed at the pressure side of the diffuser.
- Near the shroud, the flow enters the impeller at a high angle of attack, which causes a separation at about 60% from the inlet of impeller blade at the pressure side. Also a highly unsteady flow is found at the vaneless space and no separation occurs at the vaned diffuser because the separating flow near the hub try to push the flow to the shroud. The diffuser vanes periodically cut the jet flow from the impeller.

Finally, the predicted flow field was interrogated from the perspective of loss production. The only scientific measure of loss in an unsteady flow is the entropy. Figure 7 shows the instantaneous flow field entropy (s) at design flow rate at midspan. Generally, the entropy increased in the direction of flow and vortex wake leaving the impeller blade interact strongly with diffuser blade leading edge in a very complicated flow area in the vaneless space. From the figures presented above, it can be concluded that the wakes and loss are influenced by the relative location of both blades.

3. Comparison between Experimental and Numerical results

The complexity of the impeller flow as well as the inhomogeneity of the impeller discharge flow and its interaction with the flow in the diffuser make it very difficult to bring the unsteady flow field measured by the PIV with that calculated by any software together. Among those papers presented in and others, no one made a comparison between numerical and experimental unsteady flow field because it is too complicated to model theoretically and measure experimentally in the interaction region between the impeller and the diffuser. However, some comparisons are presented here to see how much the present computation method can be trusted to simulate the unsteady interaction and also to show the flow behaviors, which could not be obtained by PIV in some regions of the measured area during the measurements due to seeding problems or laser sheet accessing. It is a challenging task to bring the instantaneous unsteady absolute velocity measured by PIV to the calculated one. However, an attempt is made here to present some selected pictures for the flow in the measured area. Figures 8-10 show the comparison of the instantaneous absolute flow velocity at medium flow rate at one relative positions near the shroud, midspan and near the hub respectively. From macroscopic point of view the agreement between experimental and numerical results is good where;

1- The absolute flow velocity inside the impeller is higher than that inside the diffuser.
2- The absolute flow velocity near the shroud is a little higher than that at midspan and very small near the hub of the diffuser where a reverse flow zone pushes the flow towards the shroud.

From microscopic point of view, it must be pointed out that, there are some shortcomings of using PIV and computations, they are;

1- There is a 2mm clearance gap (which is relatively big) between impeller walls and diffuser walls along the whole circumference. This gap is a source of leakage and a highly three-dimensional flow with high axial flow velocity at the exit of the impeller along the span (from hub to shroud). The leakage of the flow with seeding in this region, make it too difficult to obtain the experimental results in this region. On the other hand, the present calculations did not consider the flow simulation in the clearance gap. The above two reasons may answer the question, why the velocity at the exit of the impeller is low from experiment and high from numerical results.
2- The regions near walls and beside the leading edge of the diffuser vanes prevent PIV laser sheets from accessing and hence the data could not be obtained at these regions. On the other hand, the computational results show an important phenomenon near the leading edge of the diffuser vanes where the proximity produced by the passing impeller and the diffuser forms a "nozzle effect". The flow rushing through the "nozzle" induces a high-level temporal acceleration that causes a rise of the lift force on the diffuser, and hence a high noise.
3- The instantaneous flow obtained from the computations are very smooth compared to the experimental results, this may be because of the turbulence model used is the standard K-ε model without any modifications (for example the effect of curvature and rotation have not taken into account). Another reason is that the real flow obtained by PIV looks like a pulsating flow with unsteady inlet and outlet boundary in contrast to the steady state boundary conditions applied to the computations. However, unsteady boundary measurement is needed especially the pressure at the exit of the diffuser.

Figure 11 shows a comparison between instantaneous flow, quasi-steady absolute velocity (the average of ten pictures at every location of the impeller) and that calculated at 165 percent flow rate at midspan. It is obvious that the average process plays an important role in smoothing the velocity vector and hence a nearer results to the numerical.

CONCLUSION

There are some of conclusions that can be drawn from the study results presented in this work.

1- In the present work, the unsteady flow in the interaction region of impeller and diffuser is measured by PIV. A low velocity region behind the blade at the exit is found at the suction side, due to formation of the wake at this region. A small vortex shedding can be observed and a highly distorted flow is observed at the vaneless space due to interaction between the rotating blades and stationary blades. Near the hub, the flow is much different than the other sections where the flow is highly unsteady and separated.

2- Two calculation models are used, Frozen/Rotor Model is used for the steady state simulation and Rotor/Stator Model is used for the transient simulation. A massive recirculation zone is found near the hub and a throughflow zone near the shroud of the diffuser resulting from the inlet of the impeller. The transient simulation predicts a highly unsteady flow region in the vaneless space between the impeller and diffuser. Also, the flow for both impeller and diffuser are much different from the hub to the shroud. Although the grid system is the same for every diffuser passage and the number of impeller blades is equal to the number of the diffuser blades, the pressure contours are not the same for every diffuser passage especially at off-design conditions due to unsteady impeller diffuser interaction. Also, the velocity field is a little different but it is not clear because it is drawn as a vector. Finally, the comparison between the unsteady measurements and unsteady calculations showed that the Rotor/Stator Model can predict the basic characteristics of unsteady flow in centrifugal fan but still need improvement to satisfy the true transient simulation for unsteady impeller diffuser interaction.

REFERENCES

[1] Inoue M. and Cumpsty N.A. 1984, " Experimental Study of Centrifugal Impeller Discharge Flow in Vaneless and Vaned Diffusers" ASME *Journal of Engineering for Gas Turbines and power* vol. 106, pp. 455-467.

[2] Sideris MT., R. A. Van DEN braembussche 1987 "Influence of a circumferential exit pressure distortion on the flow in an impeller and diffuser" *Journal of Turbomachinery*, 1987, Vol. 109, N° 1, p. 48-54.

[3] Arndt N., Acosta A.J., Brennen C.E., and Caughey T.K.,1989 " Rotor-Stator Interaction in a Diffuser Pump" ASME *Journal of Turbomachinery* vol. 111, pp. 213-221.

[4] Arndt N., Acosta A.J., Brennen C.E., and Caughey T.K.,1990 " Experimental Investigation of Rotor-Stator Interaction in a Centrifugal Pump With Several Vaned Diffusers " ASME *Journal of Turbomachinery* vol. 112, pp. 98-108.

[5] Eckardt D. " Instantaneous Measurements in the Jet-Wake Discharge Flow of a Centrifugal Compressor Impeller " ASME *Journal of Engineering for power* vol. 97,1975, pp. 337-346.

[6] Eckardt, D.,"Detailed Flow Investigations Within a High Speed Centrifugal compressor Impeller" ASME *Journal of Fluid Engineering* vol. 98,1976,pp. 390-402

[7] Rohne K.H., and Banzhaf M." Investigation of the Flow at the Exit of an Unshrouded Centrifugal Impeller and Comparison With the Classical Jet-wake Theory" ASME *Journal of Turbomachinery* vol. 113,1991, pp. 654-659.

[8] Ubaldi M., Zunino P., Barigozzi G., and Cattanei A." An Experimental Investigation of Stator Induced Unsteadiness on Centrifugal Impeller Outflow " ASME *Journal of Turbomachinery* vol. 118,1996, pp. 41-54.

[9] Krain H. 1981, " A Study on Centrifugal Impeller and Diffuser Flow" ASME *Journal of Engineering for power* vol. 103, pp. 688-697.

[10] Paone N., Riethmuller M.L., and Van den Braembussche R. A." Experimental Investigation of the Flow in the Vaneless Diffuser of a Centrifugal Pump by Particle Image Displacement Velocimetry" *Experiments in Fluids* vol. 7,1989, pp. 371-378.

[11] Humphreys W.M. and Bartman S.M. "Using Particle Image Velocimetry in Different Facilities Some Lessons Learned" AIAA paper 96-17, 1996.

[12] Wernet P.M. 1998 " Digital PIV Measurements in the Diffuser of a High Speed Centrifugal Compressor" AIAA paper, AIAA-98-2777

[13] Mekhail T., Zhang Li, Du Z.H., Chen H.P and Jansen W. " The Application of PIV in the Study of Impeller Diffuser Interaction in Centrifugal Fan. Part I –Impeller-Vaneless Diffuser Interaction " *Proceedings of The ASME Fluid Engineering Division*-IMECE2001/FED-24952 Nov.11-16, 2001 New York-USA .

[14] Mekhail T., Zhang Li, Du Z.H., Chen H.P and Jansen W. " The Application of PIV in the Study of Impeller Diffuser Interaction in Centrifugal Fan. Part I –Impeller-Vaned Diffuser Interaction " *Proceedings of The ASME Fluid Engineering Division*-IMECE2001/FED-24953 Nov.11-16, 2001 New York-USA .

[15] Kirtley K.R. and Beach T.A. " Deterministic Blade Row Interactions in a Centrifugal Compressor Stage " ASME *Journal of Turbomachinery* vol. 114,1992, pp. 304-311.

[16] Hathaway,M.D., 1990, Private Communication.

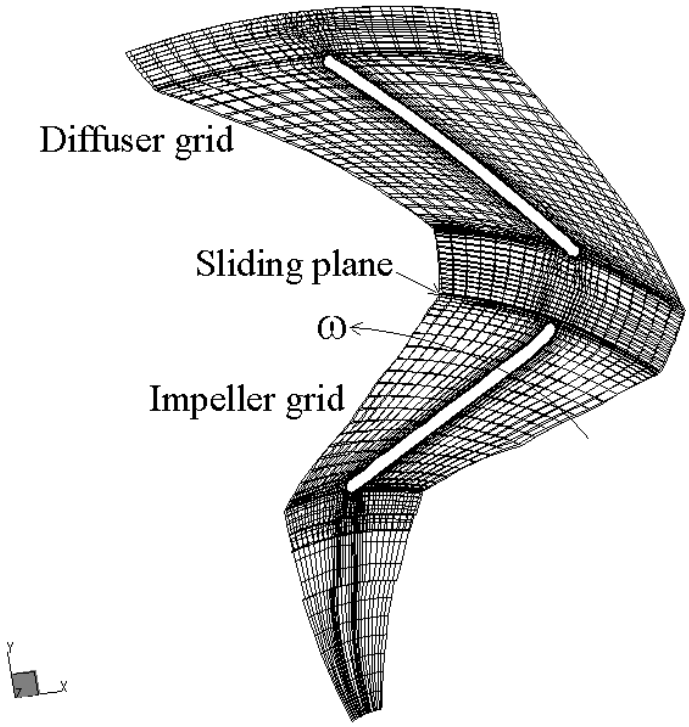

Fig. 1 The grid generated for the stage

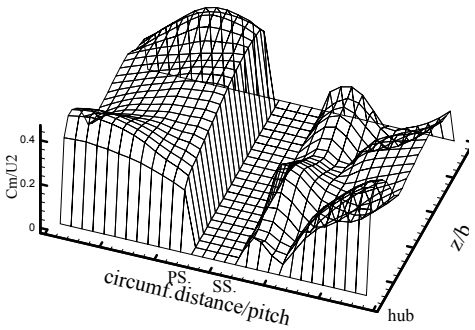

Fig. 2 Meridional velocity profile at the exit plane of the impeller

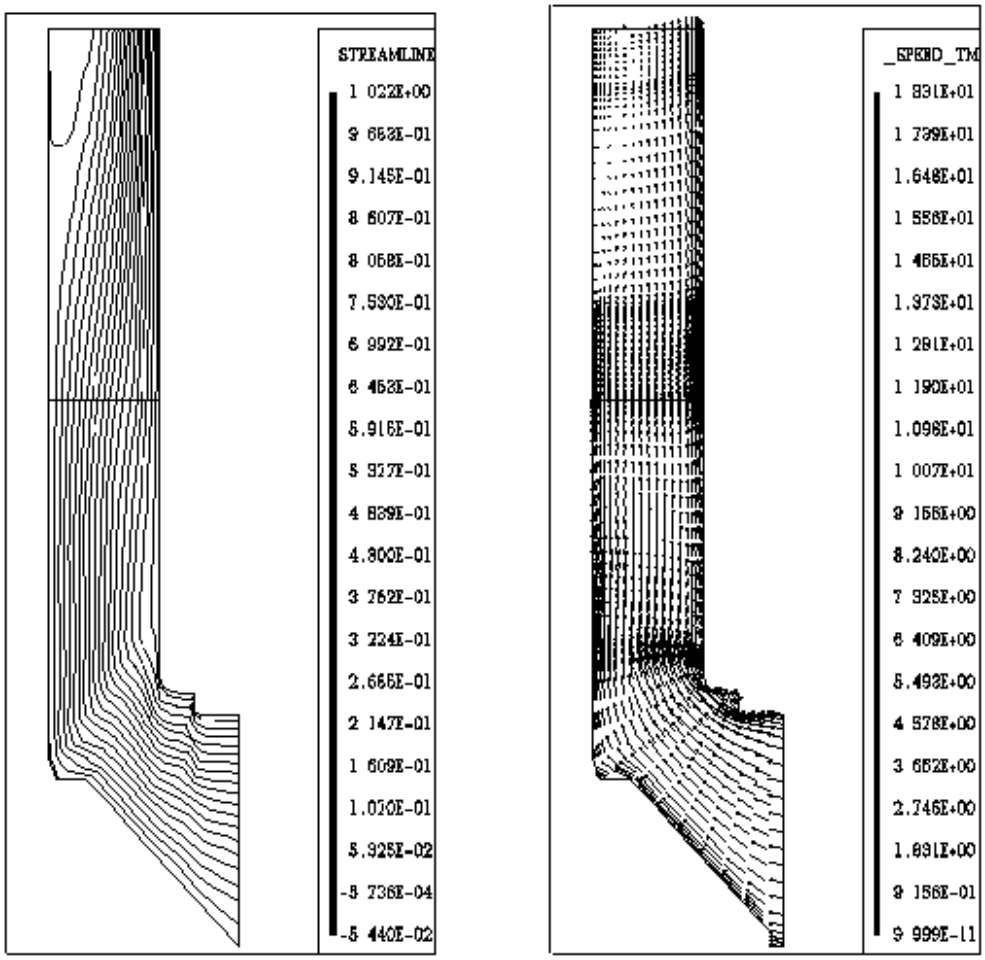

a- Stramlines b- Velocity vector

Fig. 3 Meridional symmetric flow at design flow rate

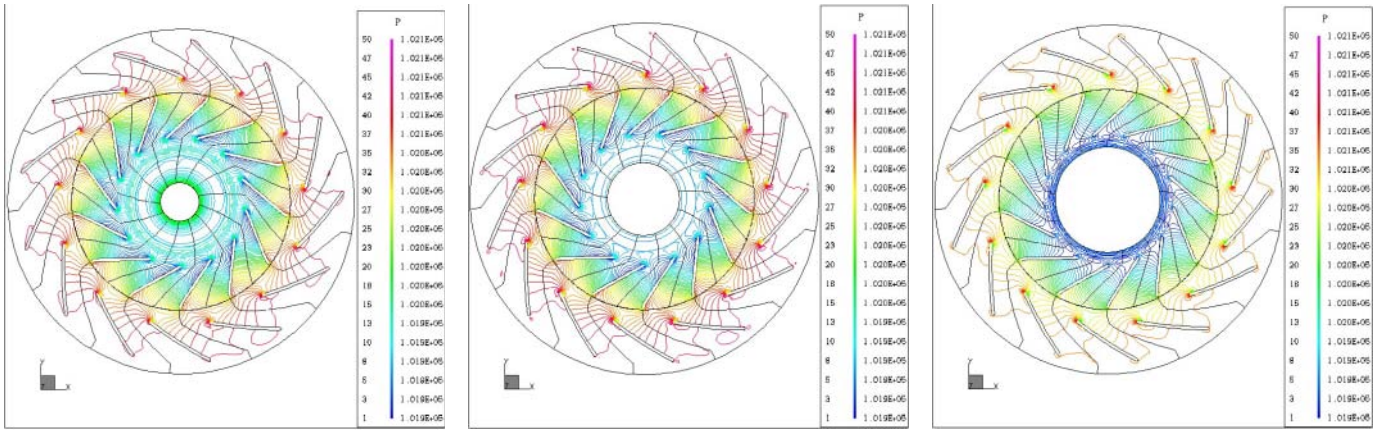

a- near the hub b- at midspan c- near the shroud

Fig. 4 Instantaneous static pressure field at design flow rate

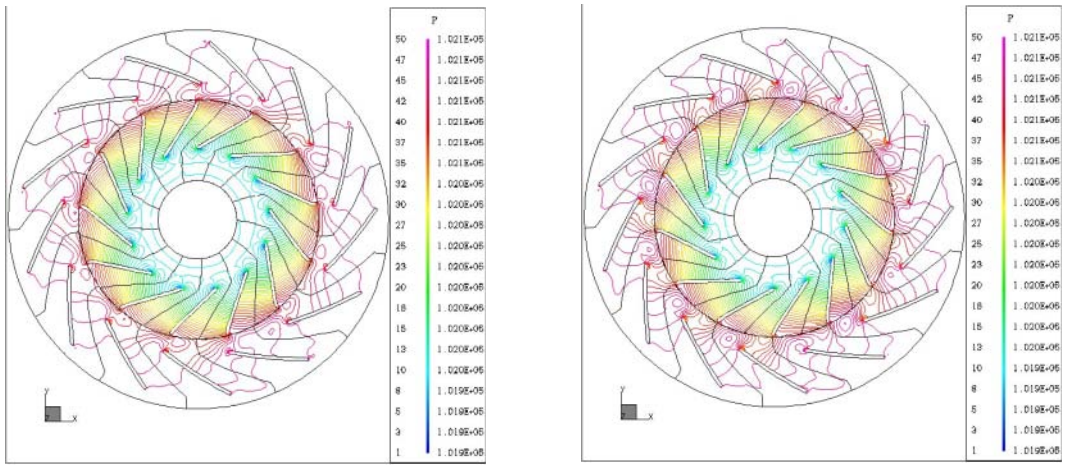

t=1 t=2

Fig. 5 Instantaneous static pressure field at 60% design flow rate at midspan

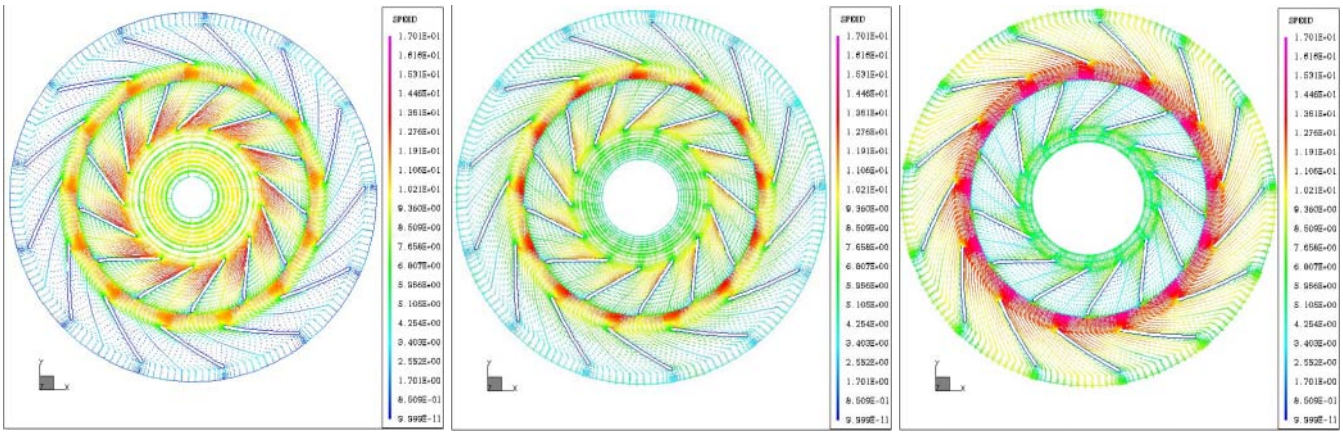

a- near the hub b- at midspan c- near the shroud

Fig. 6 Instantaneous velocity field at design flow rate

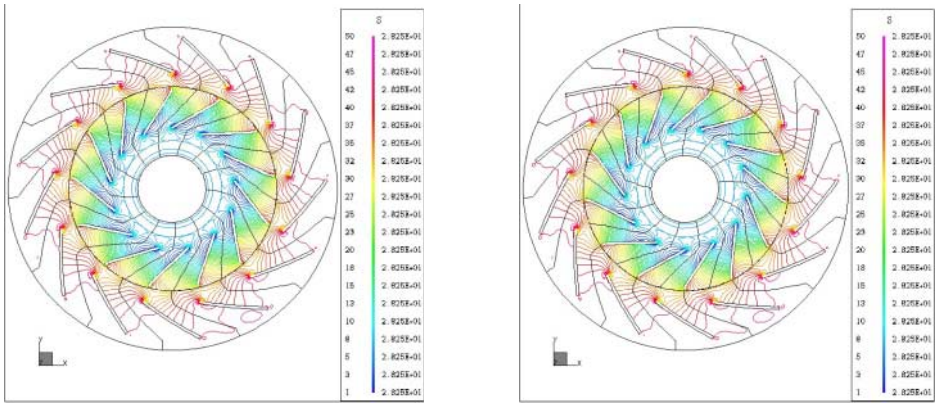

t=1 t=2

Fig. 7 Instantaneous flow field entropy at design flow rate at midspan

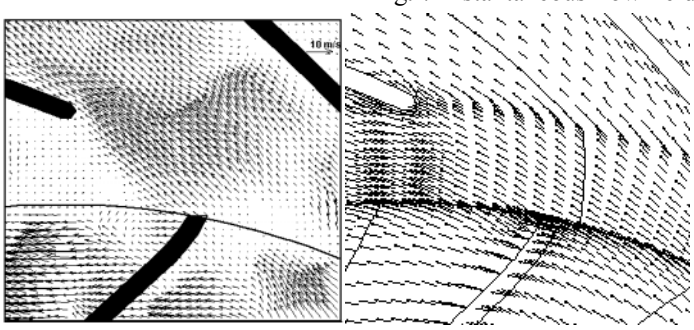

Experimental Numerical

Fig. 8 Comparison of the instantaneous absolute flow velocity at design flow rate near the shroud

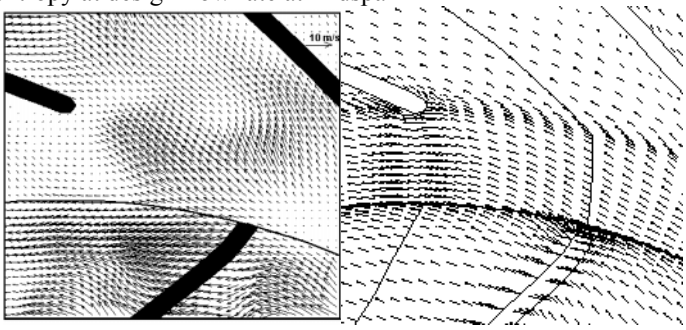

Experimental Numerical

Fig. 9 Comparison of the instantaneous absolute flow velocity at design flow rate at midspan

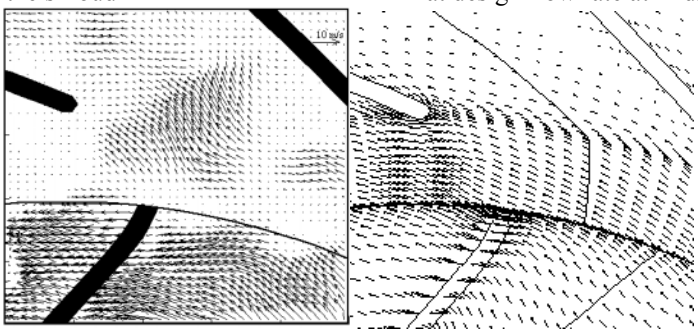

Fig. 10 Comparison of the instantaneous absolute flow velocity at design flow rate near the hub

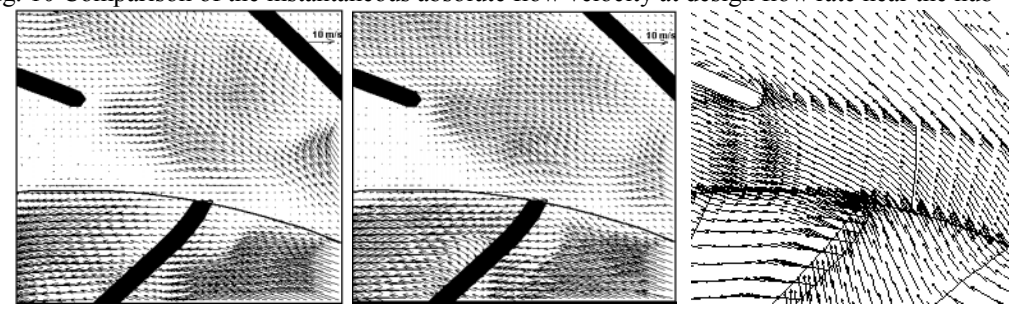

Experimental (instantaneous) Experimental (quasi-steady) Numerical

Fig. 11Comparison between instantaneous flow, quasi-steady and numerical absolute velocity at 165% design flow rate at mid span